Quantum-classical transition of the escape rate in ferrimagnetic or antiferromagnetic particles with an applied magnetic field

Bin Zhou,[1,2,*] Jiu-Qing Liang,[1,3] and Fu-Cho Pu[1,4]

[1] *State Key Laboratory of Magnetism, Institute of Physics and Center for Condensed Matter Physics, Chinese Academy of Sciences, P.O. Box 603-12, Beijing 100080, China*

[2] *Department of Physics, Hubei University, Wuhan 430062, China*

[3] *Institute of Theoretical Physics, Shanxi University, Taiyuan 030006, China*

[4] *Department of Physics, Guangzhou Normal College, Guangzhou 510400, China*

(Received 28 March 2001; published 5 September 2001)

The quantum-classical escape rate transition has been studied for ferrimagnetic or antiferromagnetic particles with an applied magnetic field along the medium axis. We derive an analytical form of the phase boundary line between first- and second-order transitions, from which phase diagrams can be obtained. It is shown that the effects of the applied magnetic field on the quantum-classical transition vary greatly for escape over the large barrier and the small barrier.

DOI: 10.1103/PhysRevB.64.132407 PACS number(s): 75.50.Xx, 75.45.+j, 03.65.Sq

The problem of the decay rate of a metastable state via quantum tunneling has profound physical implications in many fundamental phenomena in various branches of physics such as, e.g., condensed matter and particle physics and cosmology. At zero temperature the decay of the metastable states is determined by a pure quantum tunneling process whose dynamics is described by classical configurations called bounces in Euclidean space.[1] The generalization to finite-temperature tunneling has been a long-standing problem in which a new type of solution satisfying a periodic boundary condition, and therefore called the periodic instanton, was gradually realized to be relevant.[2–4] With increasing temperature thermal hopping becomes more and more important and beyond some critical or crossover temperature T_c becomes the decisive mechanism. The barrier penetration process is then governed by a static solution of the Euclidean field equation, i.e., the sphaleron. Under certain assumptions for the shape of the potential barrier, it was found that the transition between quantum tunneling and thermally assisted hopping occurs at the temperature T_c and was recognized as a smooth second-order transition in the quantum mechanical models of Affleck[5] and the cosmological models of Linde.[6] However, it was shown[7] that the smooth transition is not generic. Using a simple quantum mechanical model it was demonstrated that the time derivative of the Euclidean action would be discontinuous if the period of the instanton is not a monotonic function of energy. The sharp first-order transition occurs as a bifurcation in the plot of the action versus the period. In the context of field theory the crossover behavior and the bifurcation of periodic instantons have also been explained in a more transparent manner.[8] A sufficient criterion for the first-order phase transition in the decay problem of the metastable state was obtained by carrying out the nonlinear perturbation near the sphaleron solution in the two-dimensional string model.[9] Recently, active research on the transition behavior has been inspired, e.g., in connection with spin tunneling in condensed matter physics[10–17] and with tunneling in various field theory models.[18–23]

The phenomenon of spin tunneling has attracted considerable attention in view of a possible experiment test of the tunneling effect for mesoscopic single-domain particles, in which case it is known as macroscopic quantum tunneling. Up to now, magnetic molecular clusters have been the most promising candidates to observe macroscopic quantum coherence.[24,25] Since the first- and second-order transitions between the quantum and classical behavior of the escape rate in spin systems were introduced by Chudnovsky and Garanin,[11,26] two types of spin system, i.e., uniaxial system (such as molecular magnet $Mn_{12}Ac$) and biaxial system (such as iron cluster Fe_8), have been studied intensively.[10–17] Most theoretical studies have been focused on the ferromagnetic particle. However, considering that most ferromagnetic systems are actually ferrimagnetic particles—for instance, both $Mn_{12}Ac$ and Fe_8 are characterized by a large spin ground state which originates by incomplete compensation of antiferromagnetically coupled spins,[27]—the strong exchange interaction should be taken into consideration. In Ref. 28 Kim has treated the phase transition in ferrimagnetic or antiferromagnetic particles for two general forms of the magnetic anisotropy energy. In this paper we extend the investigation to the quantum-classical transition in a ferrimagnetic or antiferromagnetic particle with biaxial symmetry in the presence of an applied magnetic field along the medium axis. It will be shown that the effects of the applied magnetic field on the quantum-classical transition vary greatly for escape over the large barrier and the small barrier.

We consider a small ferrimagnetic or antiferromagnetic particle with two magnetic sublattices whose magnetizations $\mathbf{m}_1$ and $\mathbf{m}_2$ are coupled by the strong exchange interaction, $\mathbf{m}_1 \cdot \mathbf{m}_2/\chi_\perp$, where $\chi_\perp$ is the perpendicular susceptibility. In the case of a noncompensation of the sublattice with m $(=m_1-m_2>0)$, the Euclidean action can be taken to be[29]

$$S_E(\theta,\phi)=V\int d\tau\left\{ i\frac{m_1+m_2}{\gamma}\left(\frac{d\phi}{d\tau}\right)-i\frac{m}{\gamma}\left(\frac{d\phi}{d\tau}\right)\cos\theta + \frac{\tilde{\chi}_\perp}{2\gamma^2}\left[\left(\frac{d\theta}{d\tau}\right)^2+\left(\frac{d\phi}{d\tau}\right)^2\sin^2\theta\right]+E(\theta,\phi)\right\}, \tag{1}$$

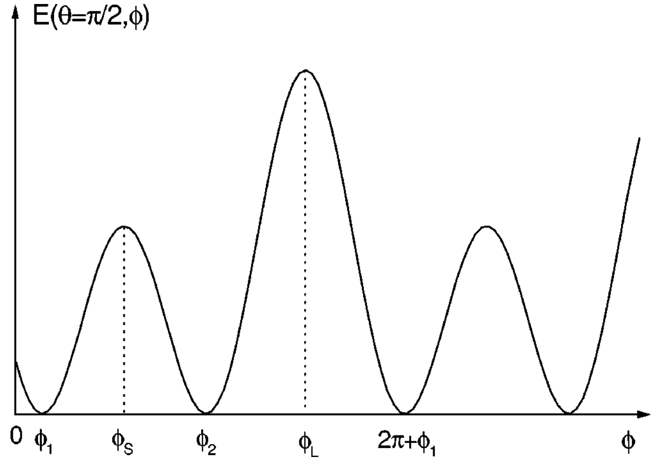

FIG. 1. The energy $E(\theta=\pi/2,\phi)$.

where V is a volume of the particle, γ the gyromagnetic ratio, and $\tilde{\chi}_\perp=\chi_\perp(m_2/m_1)$. The polar coordinate θ and the azimuthal coordinate ϕ, which are the angular components of $\mathbf{m}_1$ in the spherical coordinate system, can determine the direction of the Néel vector. The magnetocrystalline anisotropy and the Zeeman energies are included in the $E(\theta,\phi)$ term.

The system of interest has biaxial symmetry, with **x** being the easy axis, **y** being the medium axis, and **z** being the hard axis. In the presence of an external magnetic field **H** applied along the medium axis, the $E(\theta,\phi)$ term in Eq. (1) can be written as

$$E(\theta,\phi)=K_1\cos^2\theta+K_2\sin^2\theta\sin^2\phi-mH\sin\theta\sin\phi+E_0, \tag{2}$$

where K_1 and $K_2(K_1>K_2>0)$ are the transverse and longitudinal anisotopy coefficients, respectively, and E_0 is a constant which makes $E(\theta,\phi)$ zero at the initial state. When $H<H_c=2K_2/m$, the energy minima of the system are at $\theta_1=\pi/2,\phi_1=\phi_0=\arcsin(H/H_c)$ and $\theta_2=\pi/2,\phi_2=\pi-\phi_0$. Here H_c is the coercive field at which the initial state becomes classically unstable. $E(\theta=\pi/2,\phi)$ is shown in Fig. 1. The minima of the potential correspond to the equilibrium orientations of the Néel vector that resonates coherently between energetically degenerate states. These minima are separated by a small barrier S and a large barrier L. Since the configure space of this problem is a circle, only two types of tunneling paths must be taken into account. We use S to denote the tunneling path through the small barrier at $\phi_S=\pi/2$ from $\phi=\phi_1$ to $\phi=\phi_2$, and L as the tunneling path through the larger barrier at $\phi_L=3\pi/2$ from $\phi=\phi_2$ to $\phi=2\pi+\phi_1(=\phi_1)$.

The classical trajectory corresponding to the Euclidean action (1) is determined by the equations

$$-in\dot{\phi}\sin\theta+x(\ddot{\theta}-\tfrac{1}{2}\dot{\phi}^2\sin 2\theta)+\sin 2\theta(1-k\sin^2\phi)+2hk\cos\theta\sin\phi=0, \tag{3}$$

$$in\dot{\theta}+x(\ddot{\phi}\sin\theta+2\dot{\phi}\dot{\theta}\cos\theta)-2k\sin\theta\sin\phi\cos\phi+2hk\cos\phi=0, \tag{4}$$

where $n=m/(K_1\gamma)$, $x=\tilde{\chi}_\perp/(K_1\gamma^2)$, $k=K_2/K_1$, and $h=H/H_c$. Overdots denote derivatives with respect to Euclidean time τ. We note that the biaxial symmetric ferromagnetic system with an applied magnetic field along the medium axis has been discussed with the help of spin-coherent-state path integrals.[17] In Ref. 17 the field-dependent mass $M(\phi)$ is obtained. In order to restrict the mass only to be positive the condition $k(1+h)<1$ is kept for the case of escape over the large barrier. For simplicity we apply straight forward the constraint condition to discuss the ferrimagnetic or antiferromagnetic system with an applied magnetic field along the medium axis. Actually the constraint condition is justifiable. From the following Equation (8) it is seen that an unphysical singular point can justly be avoided under the constraint condition.

In the high-temperature regime two sphaleron solutions of Eqs. (3) and (4) are $(\overline{\theta}=\pi/2,\overline{\phi}_S=\pi/2)$ and $(\overline{\theta}=\pi/2,\overline{\phi}_L=3\pi/2)$, respectively. As we demonstrated above, the crossover behavior of the escape rate of this model from quantum tunneling to thermal activation can be obtained from the deviation of the period of the periodic instanton from that of the sphaleron. To this end we expand (θ,ϕ) about the sphaleron configurations $\overline{\theta}$ and $\overline{\phi}_S$ $(\overline{\phi}_L)$, i.e., for escape over the small barrier $\theta=\pi/2+\eta(\tau)$ and $\phi=\pi/2+\xi(\tau)$ and for the large barrier $\theta=\pi/2+\eta(\tau)$ and $\phi=3\pi/2+\xi(\tau)$, respectively. Denoting $\delta\Omega(\tau)\equiv(\eta(\tau),\xi(\tau))$, we have $\delta\Omega(\tau+\beta\hbar)=\delta\Omega(\tau)$ at finite temperature and write it as a Fourier series $\delta\Omega(\tau)=\Sigma_{n=-\infty}^{\infty}\delta\Omega_n\exp[i\omega_n\tau]$, where $\omega_n=2\pi n/\beta\hbar$. Since simple analysis shows that η is imaginary and ξ real, to lowest order we write them in the form $\eta\simeq ia\theta_1\sin(\omega\tau)$ and $\xi\simeq a\phi_1\cos(\omega\tau)$. Here a serves as a perturbation parameter. Substituting them into Eqs. (3) and (4) and neglecting terms of order higher than a, we obtain the relation

$$\frac{\phi_1}{\theta_1}=\frac{x\omega_\pm^2+2[1-k(1-\sigma h)]}{n\omega_\pm}=-\frac{n\omega_\pm}{x\omega_\pm^2-2k(1-\sigma h)} \tag{5}$$

and the oscillation frequency

$$\omega_\pm^2=-\frac{n^2+2[1-2k(1-\sigma h)]x}{2x^2}\pm\frac{\sqrt{n^4+4[1-2(1-\sigma h)k]n^2x+4x^2}}{2x^2}, \tag{6}$$

where $\sigma=\pm1$. Here $\sigma=+1$ corresponds to the case of escape over the small barrier and $\sigma=-1$ to the large barrier. (The prescription is also applied to the following discussion.)

Next, let us write $\eta\simeq ia\theta_1\sin(\omega\tau)+i\eta_2$, and $\xi\simeq a\phi_1\cos(\omega\tau)+\xi_2$, where η_2 and ξ_2 are of the order of a^2. Inserting them into Eqs. (3) and (4), we arrive at $\omega=\omega_+$ and $\eta_2=\xi_2=0$. In order to find the change of the oscillation period, we proceed to the third order of perturbation theory by writing $\eta \simeq ia\theta_1 \sin(\omega\tau) + i\eta_3$ and $\xi \simeq a\phi_1 \cos(\omega\tau) + \xi_3$, where η_3 and ξ_3 are of the order of a^3. Substituting them again into Eqs. (3) and (4), and retaining only terms up to $O(a^3)$, we have

$$n^4 y^2 (\omega^2 - \omega_+^2)(\omega^2 - \omega_-^2) = a^2 \frac{\phi_1^2}{4} g(k,h,y), \qquad (7)$$

where $y = x/n^2 (= \tilde{\chi}_\perp K_1/m^2)$ and

$$g(k,h,y) = \frac{2}{[1-(1-\sigma h)k]y^2} \Bigg(1-(1-\sigma h)k + [1-(1-\sigma h)k][3-2k(2-3\sigma h)]y + \frac{\sigma h k}{2}[5-8(1-\sigma h)k]y^2 - [4-(4-\sigma h)k]y^3 - \left\{ 1-(1-\sigma h)k + [1-(1-\sigma h)k](1+2\sigma h k)y - \left[2-\left(2-\frac{\sigma h}{2}\right)k\right]y^2 \right\} \times \sqrt{1+4[1-2(1-\sigma h)k]y+4y^2} \Bigg). \qquad (8)$$

Here the parameter y indicates the relative magnitude of the noncompensation. For large noncompensation ($y \ll 1$ i.e., $m \gg \sqrt{\tilde{\chi}_\perp K_1}$) and for small noncompensation ($y \gg 1$, i.e., $m \ll \sqrt{\tilde{\chi}_\perp K_1}$), the system becomes ferromagnetic and nearly compensated antiferromagnetic, respectively.[28] It is obvious that for $h=0$, Eq. (8) is reduced to Eq. (17) in Ref. 28.

As shown by Chudnovsky,[7] if the oscillation period τ is not a monotonic function of a, where a is a function of E in the absence of dissipation, the system exhibits a first-order transition. Thus, the period $\tau (=2\pi/\omega)$ in Eq. (7) should be less than $\tau_+ (=2\pi/\omega_+)$, i.e., $\omega > \omega_+$ for the first-order transition. It implies that $g(k,h,y) > 0$ in Eq. (7) for the first-order transition, and $g(k,h,y) = 0$ determines the phase boundary between the first- and second-order transitions. In this case the three parameters k, h, y should be treated simultaneously, which is not a simple problem. In the present work we will fix one parameter and then compute the boundary curve with the other two parameters. We first calculate the phase boundary lines $k(y)$'s for several values of h, which are shown in Figs. 2 and 3 for the case of the small barrier and the large one, respectively. From Fig. 2, i.e., for the case of escape over the small barrier, an immediate observation is that the first-order region for a given h diminishes as y increases, which shows the same trend as the $h=0$ case. Thus, it is evident that the region for the first-order transition is greatly reduced as the system becomes ferrimagnetic and there is no first-order transition in almost-compensated antiferromagnetic particles. The result coincides with that of Ref. 28. Figure 2 shows that the first-order region has shrunk with increasing h. For instance, the first-order region vanishes beyond $y = 1/2$, 0.172, and 0.06 for $h = 0, 0.1$, and 0.2, respectively. The effects of the applied magnetic field on the quantum-classical transition for escape over the large barrier is shown in Fig. 3 where the constraint condition $k(1+h) < 1$ has been considered. In this case, the phase boundary lines $k(y)$ shift downwards as h increases. For instance, the first-order region vanishes beyond $y = 0.576$ and 0.604 for $h = 0.1$ and 0.2, respectively. It follows that for the case of escape over the large barrier the applied magnetic field favors the occurrence of the first-order transition. This feature is opposite to that of the small barrier.

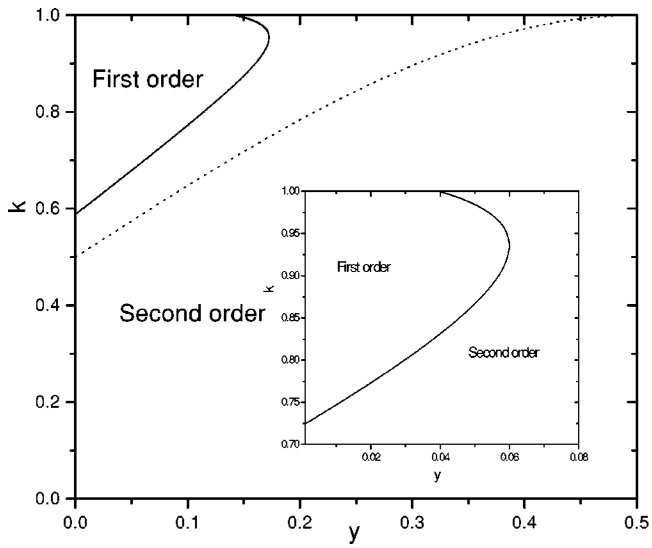

FIG. 2. Phase diagram $k(y)$ for the case of the small barrier. The solid line corresponds to $h=0.1$ and the dashed line to $h=0$. The inset corresponds to $h=0.2$.

To illustrate the above results with concrete examples, we discuss the molecular clusters Fe_8. Actually, Fe_8 is ferrimagnetic, and thereby y should be taken into account in biaxial symmetry. Take the measured value of the anisotropy parameter, e.g., $k=0.728$ for Fe_8. The phase boundary line $h(y)$

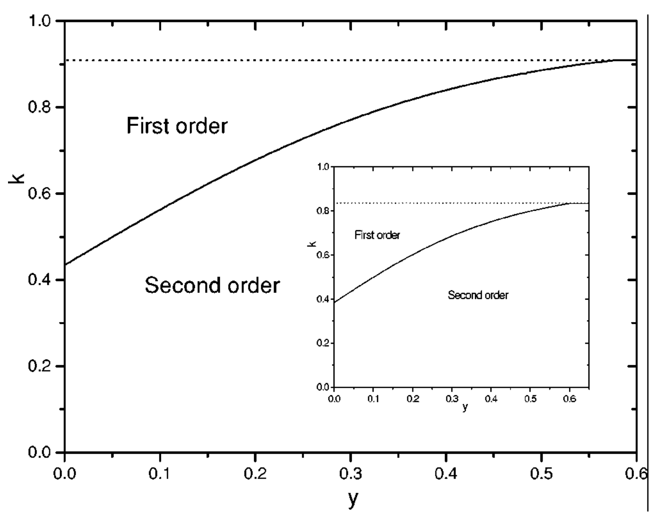

FIG. 3. Phase diagram $k(y)$ for the case of the large barrier. The solid line corresponds to $h=0.1$. The dotted line is determined by the constraint condition $k(1+h) < 1$. The inset corresponds to $h=0.2$.

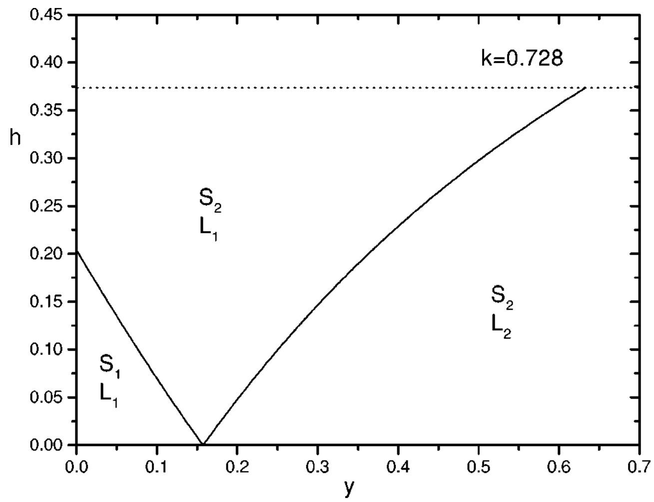

FIG. 4. Phase diagram for the orders of transition in the (y,h) plane in Fe_8 $(k=0.728)$. S_1: the first-order region for a small barrier. S_2: the second-order region for a small barrier. L_1: the first-order region for a large barrier. L_2: the second-order region for a large barrier. The dotted line is determined by the constraint condition $k(1+h)<1$.

for $k=0.728$ is shown in Fig. 4. The constraint condition $k(1+h)<1$ has been considered for the case of the large barrier. Observing Fig. 4, three types of combinations of transition are found: first-order transitions at both barriers, second-order transitions at both barriers, and a second-order transition at the small and a first-order transition at the large barrier. We note that it is not possible to have first-order transitions at the small and second-order transitions at the large barrier for any allowed values of the parameters h and y. There is a critical value $(y^*\simeq 0.157)$ at which first-order behavior turns to second-order behavior for vanishing magnetic field (i.e., $h=0$). For $y<y^*$, the large barrier exhibits only first-order transitions for any allowed values of the parameter h; for $y>y^*$, the small barrier exhibits only seconder-order transitions. For instance, when $h=0.1$, in the case of the small barrier the first-order transition can occur for $y\lesssim 0.076$ and in the case of the large barrier for $y\lesssim 0.25$.

In conclusion, we have investigated the quantum-classical escape rate transition for ferrimagnetic or antiferromagnetic particles with an applied magnetic field along the medium axis. We have derived an analytical form of the phase boundary line between first- and second-order transitions, from which phase diagrams can be obtained. It is shown that the effects of the applied magnetic field on quantum-classical transition vary greatly for escape over the large barrier and the small barrier. In the case of escape over the small barrier, the range of the first-order transition is suppressed by the applied magnetic field, while in the case of the large barrier the applied fields favor the occurrence of the first-order transition.

This work was supported by the National Nature Science Foundation of China under Grant Nos. 19775033 and 10075032.

*Corresponding author. Electronic address: binzhoucn@yahoo.com

[1] S. Coleman, Phys. Rev. D **15**, 2929 (1977); C.G. Callan, Jr. and S. Coleman, *ibid.* **16**, 1762 (1977).
[2] N.S. Manton and T.M. Samols, Phys. Lett. B **207**, 179 (1988).
[3] S.Yu. Khlebnikov, V.A. Rubakov, and P.G. Tinyakov, Nucl. Phys. B **367**, 334 (1991).
[4] J.-Q. Liang, H.J.W. Müller-Kirsten, and D.H. Tchrakian, Phys. Lett. B **282**, 105 (1992).
[5] I. Affleck, Phys. Rev. Lett. **46**, 388 (1981).
[6] A.D. Linde, Phys. Lett. B **100**, 37 (1981).
[7] E.M. Chudnovsky, Phys. Rev. A **46**, 8011 (1992).
[8] A.N. Kuznetsov and P.G. Tinyakov, Phys. Lett. B **406**, 76 (1997).
[9] D.A. Gorokhov and G. Blatter, Phys. Rev. B **56**, 3130 (1997).
[10] H.J.W. Müller-Kirsten, D.K. Park, and J.M.S. Rana, Phys. Rev. B **60**, 6662 (1999).
[11] E.M. Chudnovsky and D.A. Garanin, Phys. Rev. Lett. **79**, 4469 (1997).
[12] J.-Q. Liang, H.J.W. Müller-Kirsten, D.K. Park, and F. Zimmerschied, Phys. Rev. Lett. **81**, 216 (1998).
[13] G.H. Kim, Phys. Rev. B **59**, 11 847 (1999).
[14] D.A. Garanin, X. Martínez Hidalgo, and E.M. Chudnovsky, Phys. Rev. B **57**, 13 639 (1998).
[15] D.A. Garanin and E.M. Chudnovsky, Phys. Rev. B **59**, 3671 (1999).
[16] X. Martínez Hidalgo and E.M. Chudnovsky, J. Phys.: Condens. Matter **12**, 4243 (2000).
[17] S.Y. Lee, H.J.W. Müller-Kirsten, D.K. Park, and F. Zimmerschied, Phys. Rev. B **58**, 5554 (1998).
[18] S.Y. Lee, H. Kim, D.K. Park, and J.K. Kim, Phys. Rev. B **60**, 10 086 (1999).
[19] D.K. Park, H. Kim, and S.Y. Lee, Nucl. Phys. B **557**, 146 (1999).
[20] D.K. Park, H.J.W. Müller-Kirsten, and J.-Q. Liang, Nucl. Phys. B **578**, 728 (2000); hep-th/9910166 (unpublished).
[21] D.K. Park, S.Y. Lee, and H. Kim, Phys. Lett. B **463**, 206 (1999).
[22] J. Garriga, Phys. Rev. D **49**, 5497 (1994).
[23] A. Ferrera, Phys. Rev. D **52**, 6717 (1995).
[24] E. del Barco, N. Vernier, J.M. Hernandez, J. Tejada, E.M. Chudnovsky, E. Molins, and G. Bellessa, Europhys. Lett. **47**, 722 (1999).
[25] E. del Barco, J.M. Hernandez, J. Tejada, N. Biskup, R. Achey, I. Rutel, N. Dalal, and J. Brooks, Phys. Rev. B **62**, 3018 (2000).
[26] D.A. Garanin and E.M. Chudnovsky, Phys. Rev. B **56**, 11 102 (1997).
[27] A. Caneschi, D. Gatteschi, C. Sangregorio, R. Sessoli, L. Sorace, A. Cornia, M.A. Novak, C. Paulsen, and W. Wernsdorfer, J. Magn. Magn. Mater. **200**, 182 (1999).
[28] G.-H. Kim, Europhys. Lett. **51**, 216 (2000).
[29] E.M. Chudnovsky, J. Magn. Magn. Mater. **140-144**, 1821 (1995); B. Barbara and E.M. Chudnovsky, Phys. Lett. A **145**, 205 (1990).